



Published in final edited form as:

*Mol Cancer Res.* 2022 June 03; 20(6): 883–894. doi:10.1158/1541-7786.MCR-21-0508.

## Suppression of *SIN3A* by miR-183 promotes breast cancer metastasis

Mackenzie L. Davenport<sup>1, #</sup>, Mara R. Davis<sup>1, #</sup>, Baylea N. Davenport<sup>1</sup>, David K. Crossman<sup>1</sup>, Aaron Hall<sup>3</sup>, Jason Pike<sup>3</sup>, Shuko Harada<sup>2</sup>, Douglas R. Hurst<sup>2, \*</sup>, Mick D. Edmonds<sup>1, 2, \*</sup>

<sup>1</sup>Department of Genetics, University of Alabama at Birmingham, Birmingham, AL, USA

<sup>2</sup>Department of Pathology, University of Alabama at Birmingham, Birmingham, AL, USA

<sup>3</sup>Vulcan Informatics, Birmingham, AL, USA

### Abstract

Recent work has established that SIN3 (SWI-independent-3) chromatin modification complexes play key roles in cancer progression. We previously demonstrated that knockdown of SIN3A expression promotes human breast cancer cell invasion and metastasis; however, the levels of SIN3A in patient breast carcinoma are not known. We therefore examined SIN3A mRNA and protein in patient tissues and determined that SIN3A expression is lower in breast carcinoma relative to normal breast. Given the 3'-UTR of *SIN3A* has several conserved binding sites for oncogenic miRNA, we hypothesized that *SIN3A* is targeted by miRNA and found that ectopic miR-183 results in decreased SIN3A in breast carcinoma cell lines. Functionally, we demonstrate that miR-183 promotes breast cancer cell migration and invasion in a SIN3A-dependent manner and ectopic miR-183 promotes metastasis *in vivo*. Breast cancer patients with high levels of miR-183 and low levels of *SIN3A* have the shortest overall survival. Given the critical link between metastasis and survival in patients with breast cancer, it is of utmost importance to identify clinically relevant genes involved in metastasis. Here, we report for the first time the aberrant expression of the putative metastasis suppressing gene SIN3A in human breast cancers and propose a mechanism of SIN3A suppression by miR-183.

**Implications**—SIN3A expression is decreased in metastatic breast cancer in part due to miR-183.

### Keywords

breast cancer; microRNA; metastasis; SIN3A; miR-183

\* To whom correspondence should be addressed: Douglas R. Hurst, Department of Pathology, University of Alabama at Birmingham, Birmingham, AL 35294, douglashurst@uabmc.edu, Mick D. Edmonds, Department of Genetics, University of Alabama at Birmingham, Birmingham, AL 35294, mickedmonds@uab.edu.

# Authors contributed equally

#### Contributions

M.L.D., M.R.D., B.N.D., and M.D.E designed and conducted research. D.K.C., A.H., and J.P. acquired and performed bioinformatic analyses of data obtained from The Cancer Genome Atlas. S.H. performed patient tissue IHC analyses. M.L.D., M.R.D., D.R.H., and M.D.E analyzed and interpreted data. M.D.E. provided scientific oversight and design of all the studies. M.L.D., M.R.D., D.R.H., and M.D.E. authored the paper. All authors read, approved, and participated in the writing of the final manuscript.

#### Conflict of Interest

The authors have no conflicts of interest to report.

## Introduction

The five-year survival rate for women diagnosed with localized breast cancer in the US is 99%; a stark contrast to the less than 30% survival rate for those with distant metastasis (1). Despite the overall decrease in death rate for breast cancer patients, the median survival and rate of initial diagnosis of metastatic breast cancer has not changed substantially since 1975 (2–4). To address this problem, studies that link cellular mechanisms of cancer progression with patient data are necessary to identify relevant therapeutic targets and novel biomarkers or prognostic factors.

Over the past decade, several publications have demonstrated key roles for SIN3 (SWI-independent-3) in the processes associated with cancer progression and metastasis (5–8). SIN3 is an evolutionarily conserved nuclear scaffold protein that functions as a key regulator of gene transcription. While lacking its own intrinsic DNA binding domain, SIN3 functions through the recruitment of transcription factors, histone binding proteins, and protein modifying enzymes (9,10). SIN3 chromatin complexes, which generally serve as transcriptional repressors, have been shown to play key roles in regulating diverse biological functions including cell cycle, differentiation, proliferation, senescence, survival, energy metabolism, and embryonic development (9). The SIN3 proteins have six conserved domains: a highly conserved region (HCR), a histone deacetylase interaction domain (HID), and four paired amphipathic alpha-helix motifs (PAH), which allow them to form large SIN3 core complexes containing a multitude of interacting partner proteins, namely HDAC1, HDAC2, SAP30, SAP130, SAP180, BRMS1, and more (11). Gene duplication has given rise to two paralogs of SIN3, SIN3A and SIN3B, and knockout of either gene in mice is embryonic lethal at different stages of development (7,12,13). It is thus not surprising that studies have linked SIN3 complexes to malignancy given the fact that SIN3 has been demonstrated to play critical regulatory roles in normal biology.

Knockdown of SIN3A specifically has been shown to promote invasive morphology in breast cancer cells, induce epithelial-to-mesenchymal transition (EMT), increase breast cancer cell migration and invasion, and promote *in vivo* metastasis of human breast cancer cells in xenograft mouse models (8,14). Somatic mutation of *SIN3A* has been reported in at least one breast cancer patient, where loss of function was predicted due to cytoplasmic instead of nuclear localization. This mutation was hypothesized to contribute to breast cancer progression (15).

Despite the functional information available for the role of SIN3A in breast cancer progression *in vitro* and promotion of metastasis *in vivo* in mouse models, its expression in breast cancer patients is not known. We thus comprehensively analyzed the RNA and protein expression of this critical metastasis suppressing gene in breast cancer patients, demonstrating lowered expression in patient tumors compared to normal breast tissue. The 3'-UTR of *SIN3A* has several conserved binding sites for oncogenic miRNA, and we hypothesized that the lower expression observed in patient breast tumors is due to targeting of *SIN3A* by these oncogenic miRNA. We determined that miR-183 directly binds the *SIN3A* 3'-UTR and ectopic miR-183 results in decreased SIN3A in human breast carcinoma cell lines. miR-183 expression is higher in patient breast tumors compared to normal breast,

and its expression inversely correlates with that of *SIN3A* in human breast cancer cell lines and patients with triple-negative breast cancer (TNBC). Patients with high levels of miR-183 and low levels of *SIN3A* have the shortest overall survival, and miR-183 promotes breast cancer cell migration, invasion, and metastasis through suppression of *SIN3A*.

## Materials and methods

### Cell culture, transfections, and retroviral production and infection

T47D, ZR-75-1, MCF-7, BT-549, and SUM149 cell lines were obtained from Andra Frost (UAB). Phoenix-AMPHO, SK-BR-3, MDA-MB-231, and MCF10A cell lines were purchased from ATCC (Manassas, VA). SUM149 cells were cultured in DMEM/F12 nutrient mix (Gibco) supplemented with 5% FBS (Corning), 10ng/mL EGF (Gibco), and 10 $\mu$ g/mL bovine insulin (Cell Applications, San Diego CA). MDA-MB-231 cells were cultured in DMEM/F12 nutrient mix supplemented with 5% FBS. Phoenix-AMPHO cells were cultured following ATCC guidelines. ZR-75-1 cells were cultured in RPMI 1640 (Gibco) supplemented with 10% FBS and 10 $\mu$ g/mL of bovine insulin. BT549 cells were cultured in RPMI 1640 supplemented with 10% FBS, 10mM HEPES, 1mM sodium pyruvate, 4.5g/L glucose, and 10 $\mu$ g/mL bovine insulin. SK-BR-3 and MCF-7 cells were cultured in DMEM supplemented with 10% FBS. Cells in culture were tested bi-weekly for mycoplasma contamination by PCR analysis for mycoplasma ribosomal subunits in 70–90% confluent media supernatant. The Applied Biosystems AmpFISTR system was used to screen 15 different small tandem repeat (STR) markers to authenticate cell lines. These STR markers include those genotyped by the ATCC. Transient overexpression and knock down of miR-183 were achieved using Dharmacon (Lafayette, CO) DharmaFECT according to the manufacturer's protocol to transfect cells with either Dharmacon miR-183–5p miRIDIAN mimic or Dharmacon miR-183–5p miRIDIAN Hairpin Inhibitor. Dharmacon miRIDIAN control mimic and Dharmacon miRIDIAN Hairpin Inhibitor Negative Control were used accordingly. Transient knock down of *SIN3A* was achieved with Ambion (Austin, TX) *SIN3A* Silencer Select Pre-designed siRNA. For transfection of retroviral plasmids, Invitrogen (Carlsbad, CA) Lipofectamine 3000 Transfection Kit was used according to the manufacturer's protocol. For pLXSN and pLXSN miR-183 retroviral production, vectors were transfected into Phoenix-AMPHO cells and virus was pooled from 48, 72 and 96-hour timepoints. Breast cancer cells were infected with retrovirus containing media with 10 $\mu$ g/ml polybrene. Cells were selected with 1,200 $\mu$ g/mL G418. All cell line used in the study were passaged at least twice before experimentation was conducted.

### Migration and Invasion Assays

For migration and invasion assays, inserts were seeded with cells 24 hours post-transfection in serum free media. Migration assays were carried out using Corning (Bedford, MA) Biocoat Control Inserts with 8 $\mu$ m PET membrane. Invasion assays were carried out using ThermoScientific 8 $\mu$ m Invasion Chambers with Corning Matrigel Matrix. Both migration and invasion assays were conducted according to the manufacturer's protocol using 50,000 cells per well. 16–18hrs later transwells were stained using ThermoScientific Shandon Kwik-Diff Stain Kit according to the manufacturer's protocol. Serum containing media was used as the chemoattractant in the lower chamber of the transwells. Stained cells were

counted in four quadrants of a hemocytometer and the average number of cells per field was calculated.

### 3D Growth Assays

48-well plates were coated with 200 $\mu$ L Gibco Reduced Growth Factor Geltrex. Cell lines were resuspended in growth media supplemented with 2% Geltrex. 5,000 cells were seeded per well and fed every 4 days. Images were taken day 6 post-seeding.

### RT-qPCR

RNA was isolated from cell lines using TRIzol (ThermoFisher) according to the manufacturer's instructions. RNA was isolated from frozen patient samples using a miRNeasy kit (Qiagen). cDNA synthesis for miRNA was performed with Taqman microRNA Reverse Transcriptase kit with 10ng input RNA (ThermoFisher). TaqMan miRNA assays (ThermoFisher) were used to quantify cDNA generated from miRNA. RNU6B was the endogenous control for miRNA analysis in human tissues. 500ng of input RNA was used for cDNA synthesis of mRNA with iScript cDNA Synthesis Kit (cell lines) BioRad (Hercules, CA) and SuperScript III cDNA synthesis kit (Invitrogen) for patient samples, according to the manufacturer's instructions. SYBR Green (Qiagen) was used to quantify cDNA generated from mRNA.  $\beta$ -actin was the endogenous control for mRNA analysis. Assays were performed in triplicate. mRNA primer sequences are listed below.

#### Human qPCR Primers:

---

<i><math>\beta</math>-ACTIN</i>	Fwd: 5'- GGATGCAGAAGGAGATCA Rev: 5'- CTAGAAGCATTGCGGTG
<i>DIO2</i>	Fwd: 5'- TTCTAAGAAGGAGAAGGTGCC Rev: 5'- GCTGAGCCAAAGTTGACCA
<i>FOS</i>	Fwd: 5'- GCCTCTCTTACTACCACTACC Rev: 5'- AGATGGCAGTGACCGTGGGAAT
<i>IL24</i>	Fwd: 5'- CACAGGCGGTTTCTGCTATTC Rev: 5'- TGAACAGCATAGGAAGGGAGAC
<i>KRT81</i>	Fwd: 5'- CTATGTGAAGGCATTGGGGC Rev: 5'- CCTCCGCAGGTGGTGTTC
<i>OASL</i>	Fwd: 5'- GAGTTTCTGAGGCAGGAGC Rev: 5'- CCTGAGAACCGTGCCATTC
<i>RGS4</i>	Fwd: 5'- ACATCGGCTAGGTTTCCTGC Rev: 5'- GTGTGGGAAGAATTGTGTTTAC
<i>SIN3A</i>	Fwd: 5'- AGAGGGACACGCAGTGACGA Rev: 5'- GGCTAAGGTAGGAGGGTCGC

---

#### Cloning primers: SIN3A 3'UTR (5'nnn-3')

---

XbaI	Fwd: CTTGGATCTAGAGAAGGTAGCCAGAGCAGATAACTTGGG
SaII	Rev: TTCGTCGACTTGTCTCTGGGGTTGCCAAGAGTC

---

### Luciferase assay

The 3'UTR of *SIN3A* was cloned into a Promega (Madison, WI) pmiRGLO Luciferase miR Target Expression Vector. Primer sequences listed above. Conserved miRNA with binding sites predicted by TargetScan in the 3'UTR were tested. Briefly, HEK293-T cells were transfected using Lipofectamine 2000 with 100ng pMIR-REPORT- $\beta$ -gal, 100ng pMIR-GLO *SIN3A*, and 50nM Dharmacon miRIDIAN mimic or Scramble miR mimic. Luciferase activity was assayed 24 hours post-transfection with Promega's Dual Luciferase Reporter Assay System according to manufacturer's protocol and normalized to  $\beta$ -galactosidase expression.

### CRISPR/Cas9

sgRNA targeting miR-183 were cloned into pSpCas9(BB)-2A-GFP (PX458) vector purchased from Addgene (Watertown, MA). Targeting efficiency was validated by SURVEYOR assay. SUM149 cells were transfected with 28 $\mu$ g of either PX458 miR-183 sgRNA or PX458 EV. 48 hours post-transfection, cells were single cell sorted into 96-well plates and allowed to recover. Knockdown was determined by qPCR and editing was confirmed by Sanger sequencing.

miR-183 sgRNA: 5' TCAGTCAGTGAATTACCGAA 3'

### Target Site Blocker

A 21 nucleotide miRCURY LNA miRNA Power Target Site Blocker (TB) (Qiagen) was designed to bind to the most conserved miR-183 predicted binding site in the *SIN3A* 3'UTR (TargetScan). TSB\_ *SIN3A*\_miR-183-5p: 5'-AAGCTGGTGGATGGCACTAAG-3'. The TSB was transfected into stable miR-183 overexpressing MDA-MB-231 cells (0, 50, 100nM) using the Lipofectamine 3000 (ThermoFisher). 24hrs post-transfection TB and mock transfected cells were used for migration and invasion assays.

### Mice

For xenograft studies, 6–8 week-old female immunodeficient B6:129-Rag2tm1Fwall:R2G2 mice from Envigo (Harlan, KY) were injected into the fourth mammary fat pad (mfp) with  $2.5 \times 10^6$  MDA-MB-231 cells or into the lateral tail vein with  $1.0 \times 10^6$  cells. Tumor volume from mfp injected mice was calculated from measurements with digital calipers. At time of sacrifice, tumors were removed, weighed, and frozen. Tail vein injected mice were sacrificed 6 weeks post-injection. Lungs were collected and fixed with Bouin's solution. All animal experiments were conducted under the supervision of the UAB Animal Resources Program and according to approved institutional guidelines (IACUC #21262).

## Patient Samples

De-identified frozen breast samples (n=123) were obtained from the UAB tissue collection and banking facility, which banked samples following written informed patient consent (Clinical/pathologic details listed in Table S1). The UAB tissue collection and banking facility also provided us with an additional cohort of 71 sections from patient FFPE blocks following written informed patient consent (Clinical/pathologic details listed in Table S2). All samples were from surgical resections and were evaluated by a board-certified pathologist. All tumor samples used were determined to be >50% tumor by evaluation of H&E-stained sections. All Patient tissue studies were conducted in accordance with UAB institutional review board approval and were in accordance with recognized ethical guidelines (e.g., Declaration of Helsinki, CIOMS, Belmont Report, U.S. Common Rule).

## TCGA and METABRIC data analysis

miRNA and mRNA expression profiles for invasive breast carcinoma and normal breast tissue samples were obtained from TCGA data portal (<https://tcga-data.nci.nih.gov/tcga/>) 2020. miRNA and mRNA expression normalized reads per million (RPM) values were log<sub>2</sub> transformed prior to evaluation. mRNA microarray expression profiles from the METABRIC trial were downloaded from cBioPortal ([www.cbioportal.org/study/summary?id=brca\\_metabric](http://www.cbioportal.org/study/summary?id=brca_metabric)) 2021.

## Western blotting

Whole-cell lysates from human cell lines were generated by lysing cells with 1X RIPA buffer and Halt Protease and Phosphatase single-use Inhibitor cocktail (ThermoFisher). Human patient sample lysates were generated by lysing tissue shavings with NE-PER Nuclear and Cytoplasmic Extraction Reagents (ThermoFisher) supplemented with Halt Protease and Phosphatase single-use Inhibitor cocktail. Polyclonal rabbit SIN3A antibody was developed by 21<sup>st</sup> Century Biochemicals (Marlborough, MA) (peptide immunogen: MKKRRLDDGESDVYAAQRR-Ahx-C-amide). Other antibodies used:  $\beta$ -Actin (Sigma-Aldrich, A5441), and Histone 3 (H3) (Abcam, AB1791). Band intensities are relative to  $\beta$ -Actin (whole cell lysates) and H3 (nuclear extracts).

## Immunohistochemistry (IHC)

IHC was performed by Vanderbilt University Medical Center TPSR: 5 $\mu$ M thick sections from patient tissues were placed on the Leica Bond Max IHC stainer. All steps besides dehydration, clearing, and cover-slipping are performed on the Bond Max. Slides are deparaffinized. Heat induced antigen retrieval was performed on the Bond Max using their Epitope Retrieval 2 solution for 20 minutes. Slides were incubated with anti-SIN3A (Protocol#2383, Lot#1111780–24917, 21st Century Biochemicals, Inc., Marlboro, MA) for one hour at 1:400 dilution. The Bond Polymer Refine system was used for visualization. Slides were the dehydrated, cleared, and cover-slipped. Slides were scored by a board certified pathologist based both on their intensity (1–4) and percent positivity. Histology (H) scores were calculated per IHC slide by multiplying average intensity by percent positivity.

## Statistics

Unless otherwise stated, values represent mean  $\pm$  SEM, and 1-tailed Student's t test was used for comparisons. P values of less than 0.05 were considered significant.

## Data Availability

Data were generated by the authors and included in the article.

## Data Availability

The data that support the findings of this study are available from the last corresponding author (MDE) upon reasonable request.

## Results

### **SIN3A expression is lower in human breast tumors compared to normal breast tissue.**

SIN3A levels were evaluated in a panel of breast cancer cell lines. *SIN3A* mRNA expression was varied across the cell lines analyzed (Figure 1A). Overall, luminal cell lines expressed higher levels of *SIN3A* than HER2-enriched and TNBC cell lines, which both had lower *SIN3A* levels (1/1 and 3/4 cell lines, respectively) relative to non-tumorigenic human breast epithelial cells (MCF10A) (Figure 1A). Western blot analysis for SIN3A resulted in similar trends of expression (Figure 1B). Analysis of *SIN3A* in a cohort of frozen patient breast tumors and normal breast tissue (Clinical/pathologic details in Supplemental table S1) demonstrated that *SIN3A* expression was significantly lower in tumors compared to normal breast tissue (Mean normal = 0.000060 vs Mean tumor = 0.000034,  $p=0.001$ , student's t-test) (Figure 1C). When tumors were stratified by hormone receptor subtype, *SIN3A* expression was significantly lower across all subtypes compared to normal, with the lowest levels observed in TNBC and HER2-enriched tumors (Mean normal = 0.000060, mean luminal = 0.000038, mean TNBC = 0.000031, mean HER2 enriched = 0.000030,  $p$  values = 0.01, 0.003, 0.03, respectively) (Figure 1D). Similar findings were observed by analyzing RNA-seq expression data from The Cancer Genome Atlas (TCGA). In the TCGA cohort, we observed that *SIN3A* expression was significantly lower in breast tumors compared to normal breast tissue (Mean normal = 11.1 vs mean tumor = 10.9,  $p=0.009$ ) (Figure 1E), and the lowest levels were again noted in the TNBC and HER2-enriched subtypes (Mean normal = 11.1, Mean TNBC = 10.6, mean HER2 Enriched = 10.6,  $p$  values =  $6.1E-07$ ,  $2.2E-10$  respectively) (Figure 1F). Similar trends for decreased *SIN3A* were also observed in breast carcinoma profiled in the Molecular Taxonomy of Breast Cancer International Consortium (METABRIC) (Figure 1G–H). Luminal breast cancer *SIN3A* expression trended towards being decreased while TNBC and HER2 enriched breast cancer had significantly decreased expression when compared to normal breast. When tumors were stratified across TNM stage, *SIN3A* expression displayed opposite trends in luminal and TNBC cancers, decreasing with stage in luminal tumors and increasing with stage in TNBC tumors (Supplemental Figure 1A–B). These trends were not observed in data from TCGA or METABRIC (Supplemental Figure 1C–H) *SIN3A* protein expression was also decreased in patient TNBC tumors compared to luminal tumors by western blot (Figure 1I).

To further evaluate protein expression of SIN3A in patient tissue, we performed immunohistochemistry (IHC) for SIN3A in a second cohort of patient FFPE sections (Figure 2). Slides were scored by a board-certified pathologist (S.H.; Quantification and statistical significance Supplemental Figure 1I–J). Clinical/pathologic details are listed in Table S2. Consistent with the mRNA data, we observed strong staining for SIN3A in normal breast tissue with substantially less staining in all breast cancer subtypes examined, and the weakest staining was observed in TNBC.

The relationship between *SIN3A* expression in primary breast carcinoma and patient overall survival was evaluated. We observed a trend toward shorter overall survival in patients from the TCGA cohort with low *SIN3A* expression (median survival 34 months compared to 54 months for low and high *SIN3A* expression using the median expression of *SIN3A* as the dividing line, respectively,  $p=0.08$ , Logrank hazard ratio: 1.39, 95% CI 0.9411 – 2.052) (Figure 3A). When stratified by hormone receptor subtype, the differences in overall survival for patients with TNBC having low or high *SIN3A* expression were significantly different (median survival 24 months compared to 53 months for low and high *SIN3A* expression, respectively,  $p=0.02$ , Logrank hazard ratio: 2.32, 95% CI 0.9696 – 5.546) (Figure 3B). Overall survival of patients with luminal breast cancer was not significantly different between low and high *SIN3A* expression (Figure 3C). We also evaluated clinical outcomes in the METABRIC dataset and determined that patients with low levels of *SIN3A* in their breast carcinoma had significantly decreased relapse free survival compared to patients that had high *SIN3A* in their breast carcinoma (Supplemental Figure 2A–B).

To determine if loss of SIN3A in patient tumors occurs through copy number alterations and/or mutations, we evaluated the TCGA and METABRIC datasets. We did not observe any significant genomic alterations that would account for the decrease of SIN3A in patient breast carcinoma observed in these datasets. We found that 0.6% of the patient tumors sequenced in the METABRIC cohort ( $n=2508$ ) had amplification of *SIN3A*, and no other mutations were annotated. Likewise, in the TCGA cohort ( $n=1084$ ), we observed that less than 3% of the patient tumors sequenced had some variant of genomic alteration (amplification, deletion, missense mutation, gene fusion, truncation) similar to the dataset analyzed in the METABRIC cohort. In addition, we also evaluated the methylation levels of the promoter for *SIN3A* in normal breast and breast carcinoma. Normal breast ( $n=97$ ) had a median beta value of 0.036 and breast carcinoma ( $n=793$ ) 0.037. Beta values indicate level of DNA methylation which range from 0 (not methylated) to 1 (fully methylated). The *SIN3A* promoter has little methylation in both normal and breast carcinoma, and there is no statistically significant difference in methylation of the *SIN3A* promoter between breast carcinoma and normal breast in the TCGA dataset. Thus, other epigenetic or transcriptional mechanisms are responsible for the decreased SIN3A expression we observe in breast carcinoma.

### **SIN3A is regulated by miR-183 in breast cancer cells.**

Given the subtle decrease in SIN3A expression observed in breast cancer cell lines and patient samples, we hypothesized that a key mechanism of SIN3A downregulation is by miRNAs, which have been shown to finely tune gene expression (16–18). The 3'UTR



of *SIN3A* was cloned into a pmir-Glo luciferase miRNA target expression vector, and miRNAs predicted to target the 3'UTR by TargetScan (19) were tested for their ability to bind the 3'UTR and suppress luciferase activity (Figure 4A–B). miR-138 was previously reported to target *SIN3A* in primary cultures of human airway epithelia and thus was used as a positive control (20). miRNAs found to significantly target *SIN3A* were miR-183, miR-429, and miR-204. miR-181b was used as a negative control as it is not predicted to have target sites in the 3'UTR of *SIN3A*. Given we consistently observed the greatest decreases in luciferase activity following transfection of miR-183 mimics and *SIN3A* expression was lowest in the TNBC tumors examined, we transfected miR-183 mimic into TNBC breast cancer cell lines to determine if ectopic miR-183 would result in decreased *SIN3A* in these cells. In SUM149 breast cancer cells, ectopic expression of miR-183 reduced *SIN3A* mRNA by as much as 70%, while reducing *SIN3A* approximately 20% in MDA-MB-231 cells (Figure 4C). Ectopic expression of miR-183 also reduced *SIN3A* protein expression (Figure 4D). We did not observe changes in *SIN3A* following ectopic miR-183 expression in luminal or HER2+ breast cancer cell lines (Supplemental Figure 3A). Neither ectopic expression of miR-429 nor miR-204 significantly downregulated *SIN3A* expression in MDA-MB-231 cells (Supplemental Figure 3B). To determine if miR-183 overexpression phenocopies loss of *SIN3A*, we analyzed the mRNA expression of genes previously linked to loss of *SIN3A* (Figure 4E–F). Lewis et al. reported *DIO2*, *OASL*, *KRT81*, and *IL24* as genes that were upregulated in TNBC cell lines following knockdown of *SIN3A*. *FOS* showed intermediate upregulation, and *RGS4* was downregulated in this dataset (8). Here, we show that in MDA-MB-231 cells, overexpression of miR-183 precisely phenocopies the loss of *SIN3A* from this previous study, with upregulation of *DIO2*, *IL24*, *KRT81*, *OASL*, a more moderate increase in *FOS* expression, and down-regulation of *RGS4*. These data were validated in SUM149 cells, where expression of each gene changed correspondingly (Figure 4E). Inhibition of miR-183 coordinately reduced expression of *FOS*, *KRT81*, and *OASL* while upregulating expression of *RGS4* in BT549 breast cancer cells. Inhibiting miR-183 in SUM149 breast cancer cells also produced concordant results, downregulating *DIO2*, *FOS*, *IL24*, *KRT81*, and *OASL* while upregulating *RGS4* (Figure 4F).

### miR-183 and *SIN3A* are inversely correlated in human breast tumors.

Given that miR-183 directly targets *SIN3A* in breast cancer cells, we evaluated the expression of miR-183 in patient tissues. miR-183 was higher in patient breast tumors compared to normal breast (Figure 5A, Supplemental Figure 4A), and this overexpression occurs in all hormone receptor subtypes (Figure 5B). Analysis of miR-seq data for breast carcinoma from TCGA showed similar results for miR-183 expression (Figure 5C–D). We did not observe any significant changes in miR-183 expression across pathological stages (Supplemental Figure 4B–D). Interestingly, when the correlation between *SIN3A* and miR-183 expression was analyzed in normal human breast tissues, we observed a significant positive correlation in normal breast (simple linear regression,  $R^2 = 0.1404$ ,  $p=0.0003$ ). This correlation was less positive in the luminal and HER2-enriched subtypes compared to normal tissue and was negative in TNBC, as one might expect for a miRNA targeting an mRNA (Figure 5E). This indicated a change in the relationship between *SIN3A* and miR-183 in breast tumors compared to normal breast tissue, particularly in TNBC.

We thus analyzed the relationship of these two genes simultaneously on patient overall survival and observed the shortest median survival in patients with both low *SIN3A* and high miR-183, while the longest median survival was observed in those patients with high *SIN3A* and low miR-183 (Figure 5F). The median survival of patients with low *SIN3A*: high miR-183 expression was 24.6 months, while the median survival of those patients with high *SIN3A*: low miR-183 expression was 54.9 months, a difference of more than 2.5 years. Given these trends in survival and the published role of metastatic promotion following knockdown of *SIN3A*, we evaluated the expression of both genes in a small cohort of matched primary tumor and lymph node pairs. Higher miR-183 expression was identified in 4/5 lymph nodes compared to matched primary tumors while *SIN3A* was correspondingly down-regulated in 5/5 lymph nodes compared to matched primary tumors (Figure 5G). We also evaluated *SIN3A* target gene expression in a cohort of human breast tumors that had elevated miR-183 expression and determined that some but not all target genes for *SIN3A* changed expression as we observed above in TNBC cell lines. *DIO2* was significantly increased in only HER2 enriched tumors while *FOS* trended towards decreased expression (Supplemental Figure 5A–B). *KRT81* and *OASL* were significantly increased in both TNBC and HER2 enriched tumors, and the remaining *SIN3A* target genes had trends towards increased expression (Supplemental Figure 5C–F). Consistent with human breast cancer, miR-183 is expressed higher in mouse mammary carcinomas from MMTV-PyMT mice compared to tissue isolated from normal mammary glands (Figure 5H). As observed with patient sample analyses for *SIN3A* and miR-183, miR-183 and *SIN3A* levels were inversely correlated in TNBC cell lines compared to non-tumorigenic MCF10A cells (Figure 5I). Of the TNBC cell lines tested, 3/4 (MDA-MB-453, SUM149, BT549) had lower *SIN3A* and higher miR-183 compared to MCF10A cells. The MDA-MB-231 cells, which had increased *SIN3A* compared to MCF10A cells, had decreased miR-183 levels.

### **miR-183 promotes metastasis by targeting *SIN3A*.**

We performed a series of *in vitro* assays to determine if down-regulation of *SIN3A* by miR-183 promotes metastatic potential. In 3D growth assays, ectopic expression of miR-183 induced morphological changes in breast cancer cells. Colonies were more invasive with a greater number of and longer cellular protrusions in cells with miR-183 ectopically expressed (Figure 6A). miR-183 promoted transwell migration and invasion, while knockdown of miR-183 resulted in decreased migration and invasion in TNBC cell lines (Figure 6B, Supplemental Figure 6A–D). Endogenous expression of miR-183 in the cell lines was used as a guide for whether to overexpress or inhibit miR-183 (Figure 5I). Luminal and HER2+ cell lines were also evaluated for transwell migration after ectopic miR-183 treatment. We did not observe statistically significant increases in transwell migration resulting from ectopic miR-183 as observed in TNBC cell lines (Supplemental Figure 6E). To determine if these results were due to suppression of *SIN3A*, we designed a target site blocker oligonucleotide to selectively prevent miR-183 binding to the 3'UTR of *SIN3A*, thus allowing other targets of miR-183 to remain unaffected. Transfection of this blocking oligonucleotide resulted in decreased transwell migration and invasion of miR-183 overexpressing breast cancer cells in a dose-dependent manner (Figure 6C).

Given that ectopic expression of miR-183 promoted metastatic potential of breast cancer cells, we tested whether miR-183 could promote metastasis *in vivo*. Similar to previously published results with knockdown of *SIN3A* (8), we did not observe differences in primary tumor growth by volume or weight in an orthotopic xenograft model with overexpression of miR-183 in breast cancer cells (Figure 7A–B). There was, however, an increase in spontaneous metastases to the lungs observed from primary tumors overexpressing miR-183 (Figure 7C). To further test the role of miR-183 in promoting breast cancer metastasis, we utilized an experimental model of metastasis by injecting stable transduced cell lines into the lateral tail vein of immunocompromised mice. Once again, we observed a significant increase in lung metastases with miR-183 overexpression compared to the vector control group (Figure 7D–E). *SIN3A* levels were evaluated by qRT-PCR and determined to be significantly lower in primary tumors overexpressing miR-183 when compared to vector control tumors (Supplemental Figure 7A).

## Discussion

We demonstrate for the first time that *SIN3A* protein and mRNA levels are lower in human breast tumors compared to normal breast. This observation was consistent among all data analyzed including frozen patient tumors, FFPE tissues, TCGA RNA-seq data, and METABRIC microarray data. Within human breast cancer cell lines, *SIN3A* mRNA and protein expression were varied across the cell lines analyzed with luminal breast cancer cell lines expressing higher levels of *SIN3A* than HER2-enriched and TNBC cell lines, which both had lower *SIN3A* levels relative to non-tumorigenic human breast epithelial cells (MCF10A). We observed that *SIN3A* mRNA and protein levels corresponded in most of the cell lines analyzed, except the MDA-MB-231 cells which had high *SIN3A* transcript levels, but low protein.

To determine a potential mechanism of the observed *SIN3A* downregulation in patient tumors and cell lines, we evaluated multiple common mechanisms of gene regulation, finding no significant mutations/amplifications/deletions of *SIN3A* or changes in *SIN3A* promoter methylation. We next evaluated candidate miRNAs which were predicted to regulate *SIN3A* expression. We show that miR-183 targets *SIN3A*, reduces *SIN3A* expression in breast cancer cell lines, and promotes metastasis in human breast cancer cell lines. We also provide data that demonstrate miR-183 levels are higher in all hormone receptor subtypes of breast cancer compared to normal breast tissue, and breast cancer patients with high miR-183 and low *SIN3A* expression in their tumors have shorter overall survival. The significance of our studies is that we have unraveled a clinically relevant mechanism promoting breast cancer progression.

Recently, lower *SIN3A* expression levels in primary breast carcinoma have been shown to correlate with shorter relapse free survival (8). Similarly, we show here that lower *SIN3A* expression, likely resulting from increased miR-183 levels, in breast carcinoma results in shorter overall survival. While functional studies for *SIN3* inhibition appear to contradict the clinical data for *SIN3A*, much of the confusion surrounding the role of this chromatin modification complex in breast cancer progression has been brought on by studies that have inhibited both *SIN3* paralogs, not *SIN3A* alone (21–24). Breast cancer cells transduced with

*SIN3B* shRNA are inhibited for cell invasion and metastasis, analogous to the inhibitors that target both *SIN3* paralogs (8). Inhibition of *SIN3A* alone results in significant increases in breast cancer cell markers for EMT, cell line motility, invasion, and metastasis (8,14). Inhibiting both paralogs with shRNA in human breast cancer cells phenocopied *SIN3B* reduction. Given these data, we chose to focus our investigations on *SIN3A*, as this gene could be a metastasis suppressor, and evaluated expression and a clinically relevant mechanism of regulation associated with this specific *SIN3* paralog in human breast cancer.

The expression level of *SIN3A* in human breast cancers was lower in each of the hormonal subtypes analyzed compared to normal breast tissue; however, the lowest expression was observed in TNBC and HER2 enriched samples, and the mechanism of regulation by miR-183 appears to be most relevant in TNBC. When analyzing patient survival, the correlation of *SIN3A* expression with overall patient survival was only statistically significant in TNBC patients. This is consistent with other studies suggesting hormonal subtype specific functions of *SIN3A* (8,14,25). Our data also demonstrate an inverse correlation between miR-183 and *SIN3A* expression in TNBC. To date, there are no studies detailing the impact of hormone receptor status and *SIN3A* expression; however, *SIN3A* expression has been shown to affect estrogen signaling in the MCF7 ER $\alpha$  positive cell line, and *SIN3A* protein expression was shown to be increased by estrogen (25). While *SIN3A* was observed as having decreased levels in all breast carcinoma when compared to normal breast, we observed the smallest decrease in expression in luminal breast carcinomas, potentially due to increased ER-related signaling; however, the reason why the greatest changes in survival, expression, and miR-183-*SIN3A* functional axis were measured in TNBC remain unclear. Several mechanisms could account for this observation. For example, 1) *SIN3A* chromatin remodeling complex binding proteins could be absent or unable to complex specifically in TNBC. Supporting this, it has been shown that the lncRNA NEAT1 is estrogen-inducible and is required for FOXN3 interactions with the *SIN3A* complex (26). 2) The activation or loss of cell signaling pathways unique to TNBC could result in higher sensitivity to *SIN3A* loss or 3) Unique epigenetic modifications for TNBC allow for *SIN3A* loss to promote tumor progression. Future studies are required to elucidate detailed mechanisms to understand hormonal subtype specific functions of *SIN3A* regulating breast cancer progression.

While others have demonstrated miRNA to target *SIN3A* (20,27–29), miRNA have tissue specific function and we show for the first time *SIN3A* expression is regulated by miRNA in breast cancer cells. Our data also provide evidence for the existence of several other conserved miRNA recognition elements (MRE) located in the 3'-UTR of *SIN3A*, and we have shown direct targeting for three miRNA not previously reported. miR-183 was evaluated in these studies because ectopic miR-183 resulted in the most robust decrease of *SIN3A* in TNBC cells (Supplemental Figure 2). The majority of cell lines analyzed had linear relationships for *SIN3A* and miR-183 expression except for the MDA-MD-231 cell line which did have high *SIN3A* expression and low miR-183 levels; yet, low *SIN3A* protein. The low levels of *SIN3A* protein in the MDA-MB-231 cell line suggest alternate mechanisms of post transcriptional or translational regulation of *SIN3A* in this cell line likely exist apart from miR-183 which is not surprising. We observed increased miR-183 in patient lymph node metastases compared to primary tumors in conjunction with decreased

*SIN3A*, and patients with high miR-183 and low *SIN3A* showed the shortest survival, indicating not only does miR-183 suppress *SIN3A* in breast cancer cells *in vitro*, this is a potential mechanism for the downregulation of *SIN3A* in patients. miR-183 has previously been reported as highly expressed in breast tumors compared to normal breast tissue, high expression linked to shorter overall and disease-free survival (DFS), and overexpression leads to increased migration and invasion of breast cancer cells *in vitro* (30–33). These published datasets are highly consistent with our data. We also evaluated *SIN3A* target gene expression in a cohort of human breast tumors that had elevated miR-183 expression and determined that only *KRT81* and *OASL* significantly increased expression as observed in TNBC cell lines, while *DIO2* trended up.

We also evaluated for the first time the overexpression of miR-183 in breast cancer cells *in vivo* and show an increase in metastasis. This is also the first time overexpression of miR-183 has been linked to suppression of *SIN3A*, demonstrating the relevance of the miR-183-*SIN3A* axis promoting TNBC metastasis.

In summary, our results demonstrate a novel mechanism for the downregulation of a critical metastasis suppressing gene in breast cancer patients. Understanding these key pathways is of paramount importance for designing new therapeutic approaches or identifying prognostic biomarkers in breast cancer. Targeting the miR-183-*SIN3A* axis may provide a novel approach towards treating metastatic disease. New technologies not previously available now allow for miRNA delivery and knockdown in breast cells (34). Inhibition of miR-183 or restoration of *SIN3A* in TNBC are future areas of investigation that may bring major advances toward the treatment of metastatic disease.

## Supplementary Material

Refer to Web version on PubMed Central for supplementary material.

## Funding:

This work was supported by T32 Predoctoral Fellowship NIH 5T32GM008111-32 (MLD), American Cancer Society Institutional Research Grant award number IRG-18-162-59 (MDE), National Cancer Institute Cancer Center Support Grant award number P30 CA013148 Pilot Award (MDE), METAvivor Early Career Investigator Award (MDE).

## References

1. Siegel RL, Miller KD, Fuchs HE, Jemal A. Cancer Statistics, 2021. *CA Cancer J Clin* 2021 doi 10.3322/caac.21654.
2. Welch HG, Gorski DH, Albertsen PC. Trends in Metastatic Breast and Prostate Cancer--Lessons in Cancer Dynamics. *N Engl J Med* 2015;373(18):1685–7 doi 10.1056/NEJMp1510443. [PubMed: 26510017]
3. Caswell-Jin JL, Plevritis SK, Tian L, Cadham CJ, Xu C, Stout NK, et al. Change in Survival in Metastatic Breast Cancer with Treatment Advances: Meta-Analysis and Systematic Review. *JNCI Cancer Spectr* 2018;2(4):pky062 doi 10.1093/jncics/pky062. [PubMed: 30627694]
4. Tevaarwerk AJ, Gray RJ, Schneider BP, Smith ML, Wagner LI, Fetting JH, et al. Survival in patients with metastatic recurrent breast cancer after adjuvant chemotherapy: little evidence of improvement over the past 30 years. *Cancer* 2013;119(6):1140–8 doi 10.1002/cncr.27819. [PubMed: 23065954]

5. Das TK, Sangodkar J, Negre N, Narla G, Cagan RL. Sin3a acts through a multi-gene module to regulate invasion in *Drosophila* and human tumors. *Oncogene* 2013;32(26):3184–97 doi 10.1038/onc.2012.326. [PubMed: 22890320]
6. Farias EF, Petrie K, Leibovitch B, Murtagh J, Chornet MB, Schenk T, et al. Interference with Sin3 function induces epigenetic reprogramming and differentiation in breast cancer cells. *Proc Natl Acad Sci U S A* 2010;107(26):11811–6 doi 10.1073/pnas.1006737107. [PubMed: 20547842]
7. Dannenberg JH, David G, Zhong S, van der Torre J, Wong WH, Depinho RA. mSin3A corepressor regulates diverse transcriptional networks governing normal and neoplastic growth and survival. *Genes Dev* 2005;19(13):1581–95 doi 10.1101/gad.1286905. [PubMed: 15998811]
8. Lewis MJ, Liu J, Libby EF, Lee M, Crawford NP, Hurst DR. SIN3A and SIN3B differentially regulate breast cancer metastasis. *Oncotarget* 2016;7(48):78713–25 doi 10.18632/oncotarget.12805. [PubMed: 27780928]
9. Kadamb R, Mittal S, Bansal N, Batra H, Saluja D. Sin3: insight into its transcription regulatory functions. *Eur J Cell Biol* 2013;92(8–9):237–46 doi 10.1016/j.ejcb.2013.09.001. [PubMed: 24189169]
10. Silverstein RA, Ekwall K. Sin3: a flexible regulator of global gene expression and genome stability. *Curr Genet* 2005;47(1):1–17 doi 10.1007/s00294-004-0541-5. [PubMed: 15565322]
11. Chaubal A, Pile LA. Same agent, different messages: insight into transcriptional regulation by SIN3 isoforms. *Epigenetics Chromatin* 2018;11(1):17 doi 10.1186/s13072-018-0188-y. [PubMed: 29665841]
12. Cowley SM, Iritani BM, Mendrysa SM, Xu T, Cheng PF, Yada J, et al. The mSin3A chromatin-modifying complex is essential for embryogenesis and T-cell development. *Mol Cell Biol* 2005;25(16):6990–7004 doi 10.1128/MCB.25.16.6990-7004.2005. [PubMed: 16055712]
13. David G, Grandinetti KB, Finnerty PM, Simpson N, Chu GC, Depinho RA. Specific requirement of the chromatin modifier mSin3B in cell cycle exit and cellular differentiation. *Proc Natl Acad Sci U S A* 2008;105(11):4168–72 doi 10.1073/pnas.0710285105. [PubMed: 18332431]
14. Yang Y, Huang W, Qiu R, Liu R, Zeng Y, Gao J, et al. LSD1 coordinates with the SIN3A/HDAC complex and maintains sensitivity to chemotherapy in breast cancer. *J Mol Cell Biol* 2018;10(4):285–301 doi 10.1093/jmcb/mjy021. [PubMed: 29741645]
15. Watanabe K, Yamamoto S, Sakaguti S, Isayama K, Oka M, Nagano H, et al. A novel somatic mutation of SIN3A detected in breast cancer by whole-exome sequencing enhances cell proliferation through ERalpha expression. *Sci Rep* 2018;8(1):16000 doi 10.1038/s41598-018-34290-1. [PubMed: 30375428]
16. Filipowicz W, Bhattacharyya SN, Sonenberg N. Mechanisms of post-transcriptional regulation by microRNAs: are the answers in sight? *Nat Rev Genet* 2008;9(2):102–14 doi 10.1038/nrg2290. [PubMed: 18197166]
17. Ebert MS, Sharp PA. Roles for microRNAs in conferring robustness to biological processes. *Cell* 2012;149(3):515–24 doi 10.1016/j.cell.2012.04.005. [PubMed: 22541426]
18. Feeley KP, Edmonds MD. Hiding in Plain Sight: Rediscovering the Importance of Noncoding RNA in Human Malignancy. *Cancer Res* 2018;78(9):2149–58 doi 10.1158/0008-5472.CAN-17-2675. [PubMed: 29632135]
19. Agarwal V, Bell GW, Nam JW, Bartel DP. Predicting effective microRNA target sites in mammalian mRNAs. *Elife* 2015;4 doi 10.7554/eLife.05005.
20. Ramachandran S, Karp PH, Jiang P, Ostedgaard LS, Walz AE, Fisher JT, et al. A microRNA network regulates expression and biosynthesis of wild-type and DeltaF508 mutant cystic fibrosis transmembrane conductance regulator. *Proc Natl Acad Sci U S A* 2012;109(33):13362–7 doi 10.1073/pnas.1210906109. [PubMed: 22853952]
21. Bansal N, Bosch A, Leibovitch B, Pereira L, Cubedo E, Yu J, et al. Blocking the PAH2 domain of Sin3A inhibits tumorigenesis and confers retinoid sensitivity in triple negative breast cancer. *Oncotarget* 2016;7(28):43689–702 doi 10.18632/oncotarget.9905. [PubMed: 27286261]
22. Kwon YJ, Leibovitch BA, Bansal N, Pereira L, Chung CY, Ariztia EV, et al. Targeted interference of SIN3A-TGIF1 function by SID decoy treatment inhibits Wnt signaling and invasion in triple negative breast cancer cells. *Oncotarget* 2017;8(51):88421–36 doi 10.18632/oncotarget.11381. [PubMed: 29179446]

23. Bansal N, Petrie K, Christova R, Chung CY, Leibovitch BA, Howell L, et al. Targeting the SIN3A-PF1 interaction inhibits epithelial to mesenchymal transition and maintenance of a stem cell phenotype in triple negative breast cancer. *Oncotarget* 2015;6(33):34087–105 doi 10.18632/oncotarget.6048. [PubMed: 26460951]
24. Kwon YJ, Petrie K, Leibovitch BA, Zeng L, Mezei M, Howell L, et al. Selective Inhibition of SIN3 Corepressor with Avermectins as a Novel Therapeutic Strategy in Triple-Negative Breast Cancer. *Mol Cancer Ther* 2015;14(8):1824–36 doi 10.1158/1535-7163.MCT-14-0980-T. [PubMed: 26078298]
25. Ellison-Zelski SJ, Alarid ET. Maximum growth and survival of estrogen receptor-alpha positive breast cancer cells requires the Sin3A transcriptional repressor. *Mol Cancer* 2010;9:263 doi 10.1186/1476-4598-9-263. [PubMed: 20920219]
26. Li W, Zhang Z, Liu X, Cheng X, Zhang Y, Han X, et al. The FOXN3-NEAT1-SIN3A repressor complex promotes progression of hormonally responsive breast cancer. *J Clin Invest* 2017;127(9):3421–40 doi 10.1172/JCI94233. [PubMed: 28805661]
27. Shang C, Hong Y, Guo Y, Liu YH, Xue YX. MiR-210 up-regulation inhibits proliferation and induces apoptosis in glioma cells by targeting SIN3A. *Med Sci Monit* 2014;20:2571–7 doi 10.12659/MSM.892994. [PubMed: 25481483]
28. Chou C-H, Yang M-H. Twist1 induces the expression of microRNA-29 to suppress SIN3A in head and neck cancer cells. *Journal of Cancer Research and Practice* 2016;3(4):113–7 doi 10.1016/j.jcrpr.2016.03.002.
29. Ren J, Li X, Dong H, Suo L, Zhang J, Zhang L, et al. miR-210-3p regulates the proliferation and apoptosis of non-small cell lung cancer cells by targeting SIN3A. *Exp Ther Med* 2019;18(4):2565–73 doi 10.3892/etm.2019.7867. [PubMed: 31555365]
30. Song C, Zhang L, Wang J, Huang Z, Li X, Wu M, et al. High expression of microRNA-183/182/96 cluster as a prognostic biomarker for breast cancer. *Sci Rep* 2016;6:24502 doi 10.1038/srep24502. [PubMed: 27071841]
31. Li Y, Zeng Q, Qiu J, Pang T, Ye F, Huang L, et al. MiR-183-5p Promotes Proliferation, Metastasis and Angiogenesis in Breast Cancer Cells through Negatively Regulating Four and a Half LIM Protein 1. *J Breast Cancer* 2020;23(4):355–72 doi 10.4048/jbc.2020.23.e47. [PubMed: 32908787]
32. Li P, Sheng C, Huang L, Zhang H, Huang L, Cheng Z, et al. MiR-183/-96/-182 cluster is up-regulated in most breast cancers and increases cell proliferation and migration. *Breast Cancer Res* 2014;16(6):473 doi 10.1186/s13058-014-0473-z. [PubMed: 25394902]
33. Cheng Y, Xiang G, Meng Y, Dong R. MiRNA-183-5p promotes cell proliferation and inhibits apoptosis in human breast cancer by targeting the PDCD4. *Reprod Biol* 2016;16(3):225–33 doi 10.1016/j.repbio.2016.07.002. [PubMed: 27476679]
34. Orellana EA, Kasinski AL. No vehicle, no problem. *Oncotarget* 2017;8(57):96470–1 doi 10.18632/oncotarget.22100. [PubMed: 29228541]

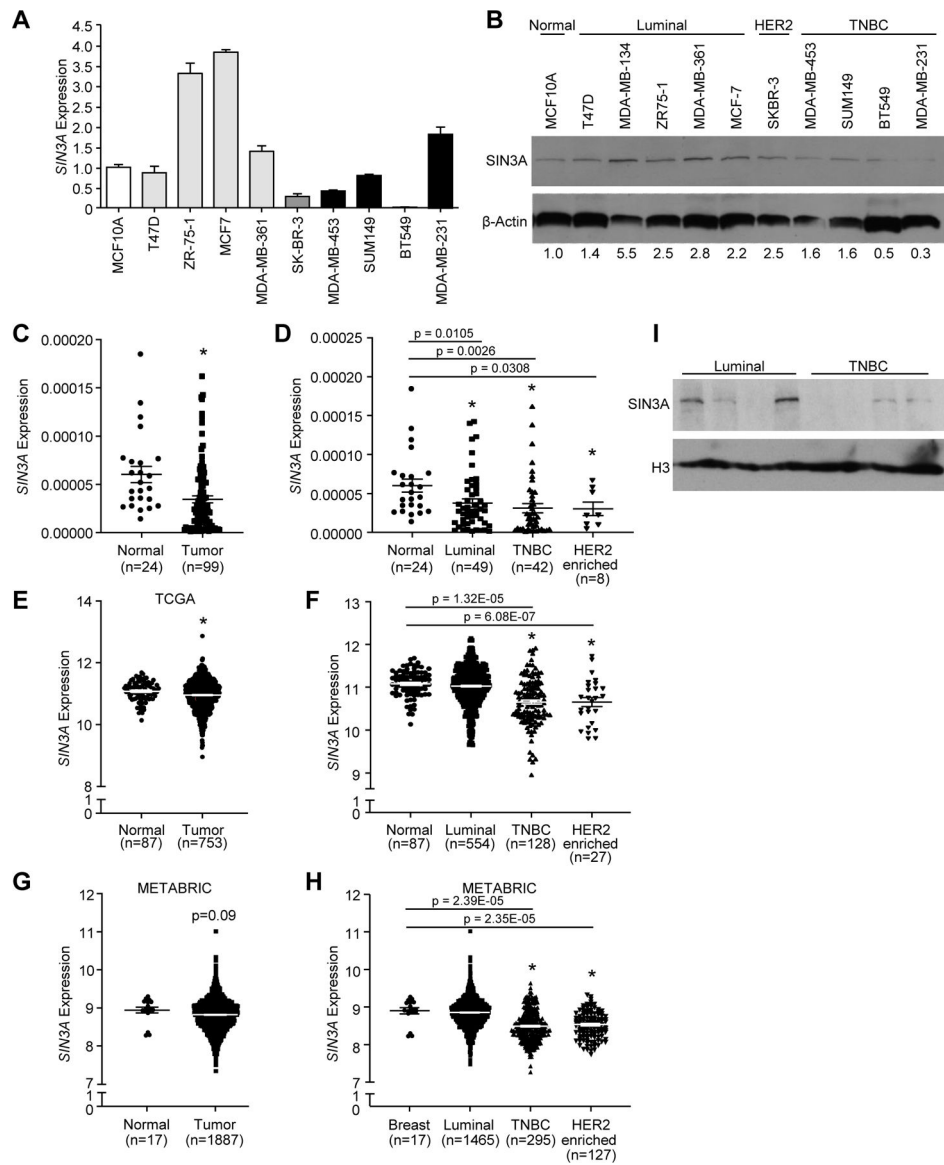


**Figure 1. SIN3A expression is decreased in human breast cancer and breast cancer cell lines.** (A, C-D) *SIN3A* levels determined by qRT-PCR. Expression normalized to  $\beta$ -Actin (A) cell lines (C-D) patient samples. Mean *SIN3A* expression (Error bars  $\pm$  SEM: \* $p < 0.05$ , student's t-test). Number (n) samples indicated (B) Western blot for *SIN3A*, whole cell lysates from breast cancer cell lines. Data are representative of 3 independent experiments. (E-F) *SIN3A* RNA-seq data from TCGA, log<sub>2</sub>-transformed normalized reads per million. Mean *SIN3A* expression (Error bars  $\pm$  SEM: \* $p < 0.05$ , student's t-test). (G-H) *SIN3A* microarray data from METABRIC. Mean *SIN3A* expression (Error bars  $\pm$  SEM: \* $p < 0.05$ , student's t-test). (I) Western blot for *SIN3A*, nuclear extracts from patient samples.



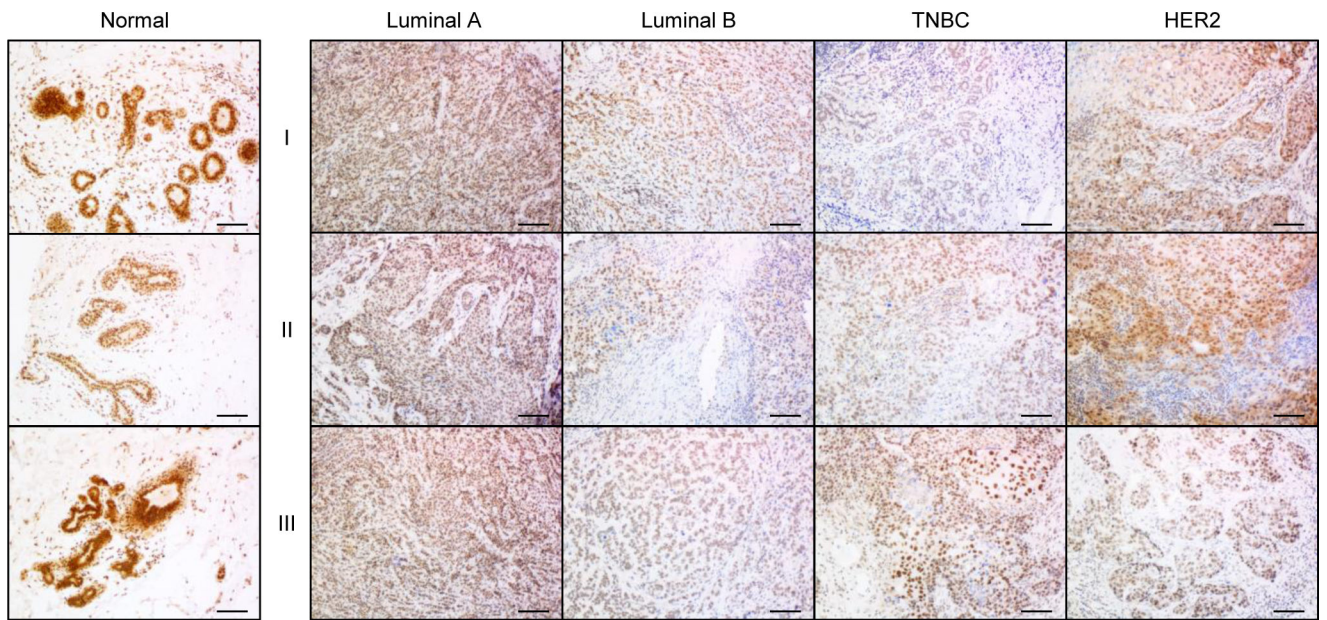


**Figure 2. SIN3A expression is decreased in human breast cancer.** IHC staining of normal breast tissue and patient breast tumors from each hormone receptor subtype. Representative images shown, 20X. Scale bar = 0.1mm

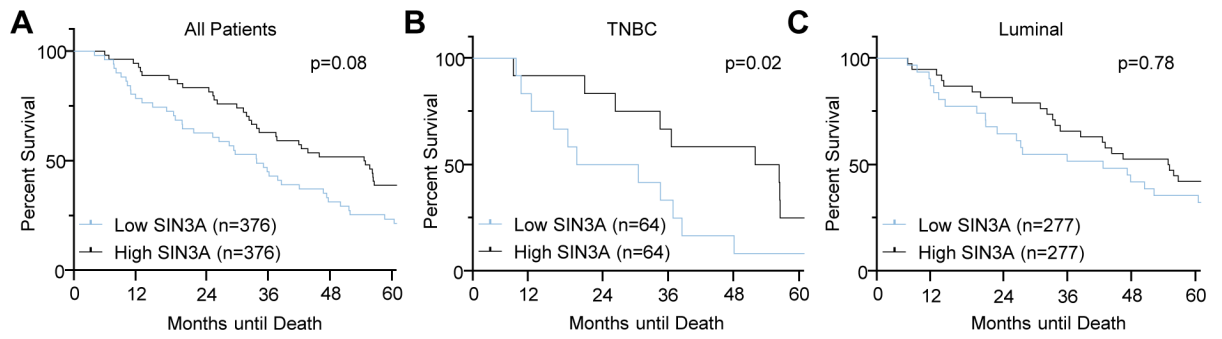


**Figure 3. *SIN3A* expression correlates with patient survival in triple-negative breast cancer.** (A-C) Kaplan-Meier survival plots for *SIN3A* expression in uncensored TCGA RNA-seq breast cancer data divided by median expression. P values were determined by log-rank test.

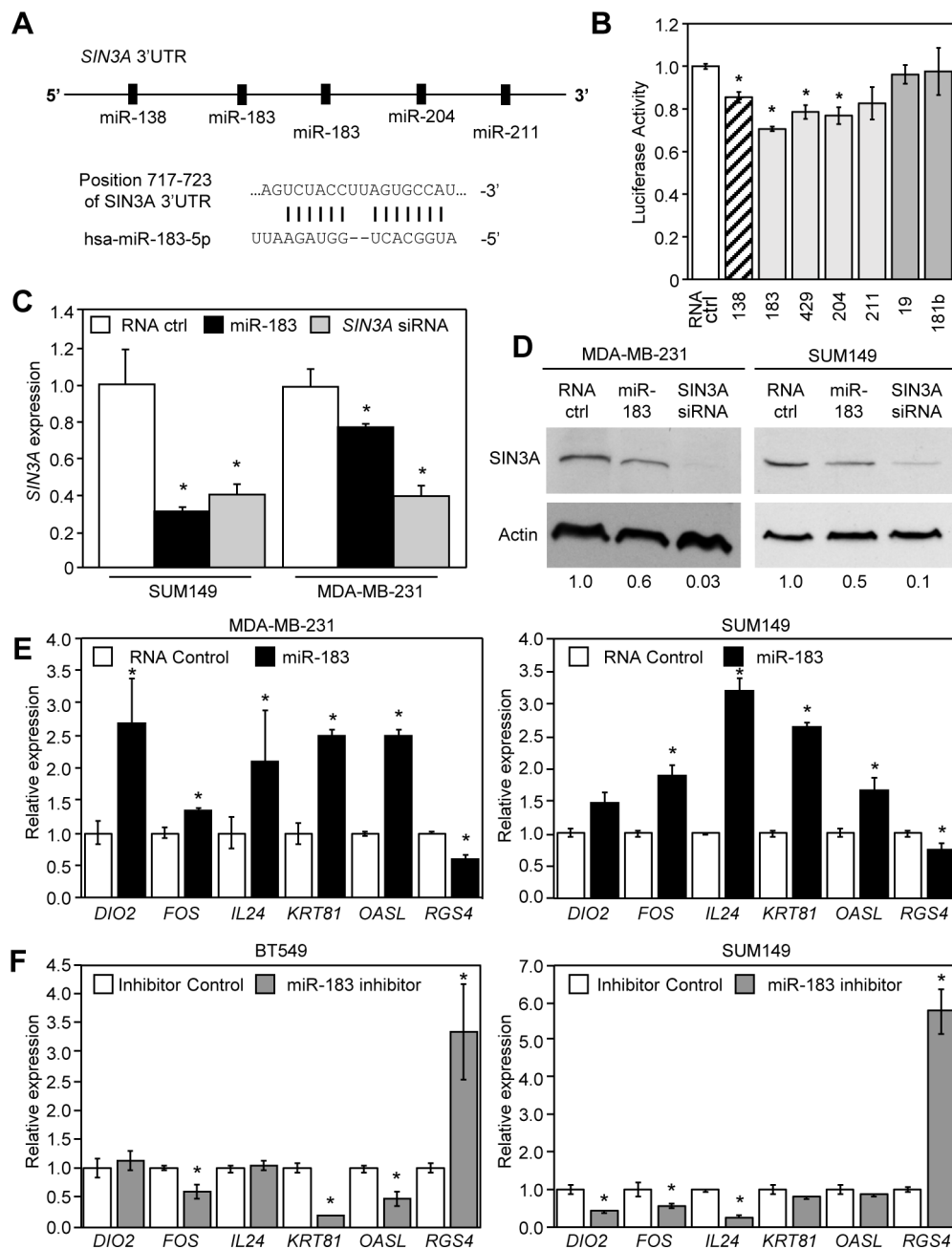


**Figure 4. *SIN3A* is regulated by miR-183 in breast cancer cells.**

(A) Diagram of *SIN3A* 3'UTR and TargetScan predicted miRNAs. Alignment of hsa-miR-183-5p seed sequence with *SIN3A* 3'UTR. (B) Relative luciferase activity in HEK293-T cells transfected with reporter plasmid and miRNA mimics indicated. Activity normalized to  $\beta$ -galactosidase. (C) *SIN3A* levels determined by qRT-PCR following transfection with RNA control, miR-183 mimic, or *SIN3A* siRNA. Expression normalized to  $\beta$ -Actin. Data are representative of at least 3 independent experiments. Mean expression, technical triplicates (Error bars  $\pm$  SEM; \* $p$ <0.05, student's t-test). (D) Western blot for *SIN3A* following transfection with RNA control, miR-183 mimic, or *SIN3A* siRNA. Loading control  $\beta$ -Actin, densitometry values below. (E-F) Relative gene expression determined by

qRT-PCR following miR-183 mimic (E) or miR-183 inhibitor (F) transfection. Expression normalized to  $\beta$ -Actin. Data are representative of at least 3 independent experiments. Mean expression, technical triplicates (Error bars  $\pm$  SEM: \* $p < 0.05$ , student's t-test).

Author Manuscript

Author Manuscript

Author Manuscript

Author Manuscript

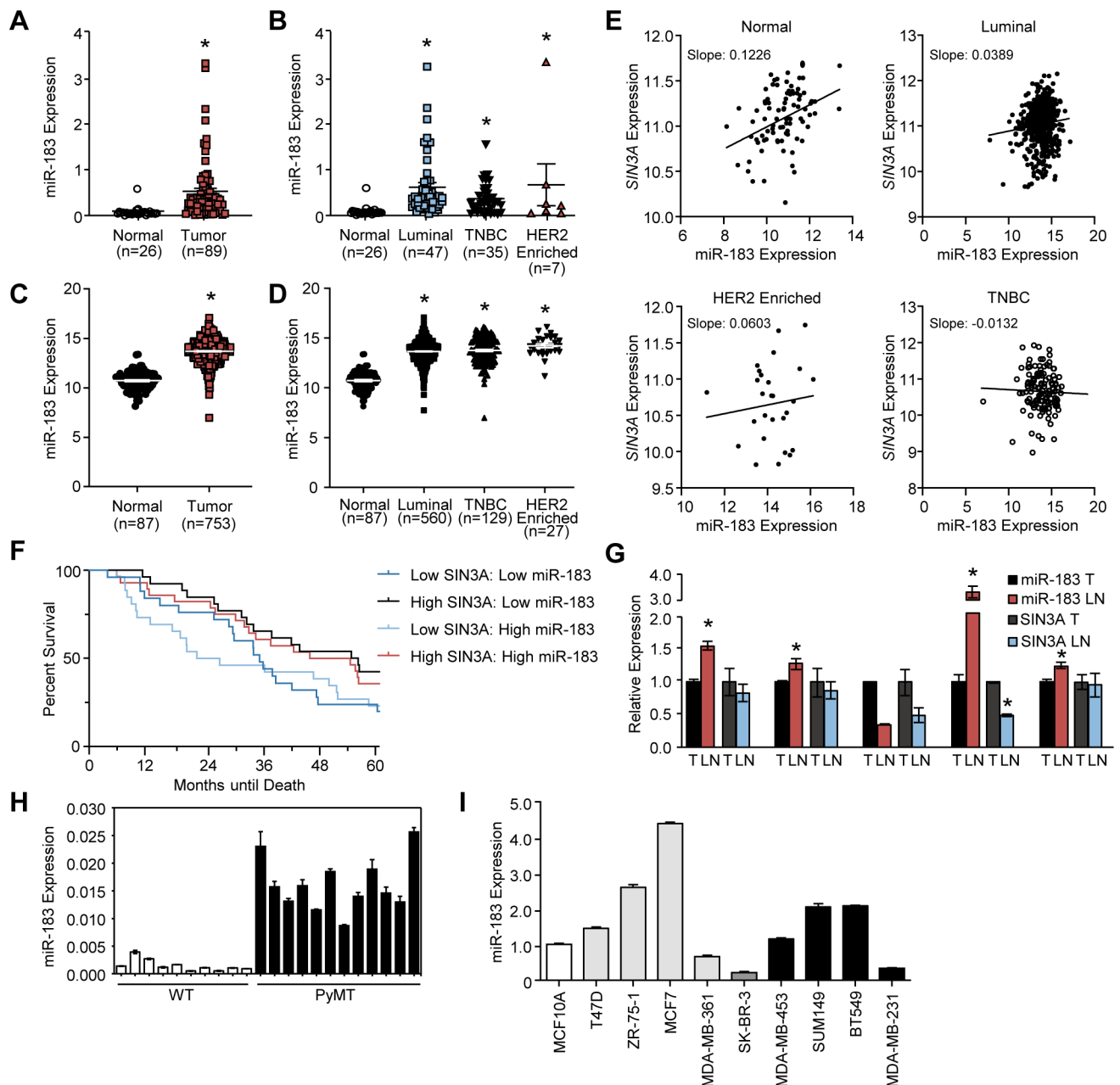


**Figure 5. miR-183 targets SIN3A in human breast cancer.**

(A-B) miR-183 levels determined by qRT-PCR. Expression normalized to endogenous control RNU6B (A) normal breast vs primary tumor (B) normal breast vs hormone receptor subtypes. (C-D) miR-183 miR-seq data from TCGA, log<sub>2</sub>-transformed normalized reads per million. Mean miR-183 expression (Error bars  $\pm$  SEM; \* $p < 0.05$ , student's t-test). Number (n) samples indicated. (E) Simple linear regression of miR-183 and *SIN3A* expression in patients from the TCGA data portal. (F) Kaplan-Meier survival plot for *SIN3A* and miR-183 expression in uncensored TCGA breast cancer data divided by median expression. High *SIN3A*: low miR-183 vs Low *SIN3A*: high miR-183 ( $p = 0.23$ , Logrank hazard ratio: 0.729, 95% CI 0.4203 – 1.264). P values were determined by log-rank test.

LL n=25, HL n=26, LH n=26, HH n=28 (G) miR-183 and *SIN3A* levels determined by qRT-PCR in matched tumor and lymph node pairs from breast cancer patients. miR-183 expression normalized to RNU6B. *SIN3A* expression normalized to  $\beta$ -Actin. Primary tumor (T), lymph node metastases (LN). (H) Mouse miR-183 levels determined with qRT-PCR in littermate matched wild type FVB mammary gland and PyMT mammary tumors. Expression normalized to endogenous control sno-202. Mean expression (Error bars  $\pm$  SEM). (I) miR-183 levels determined by qRT-PCR. Expression normalized to endogenous control RNU6B. Data are representative of two independent experiments.

Author Manuscript

Author Manuscript

Author Manuscript

Author Manuscript

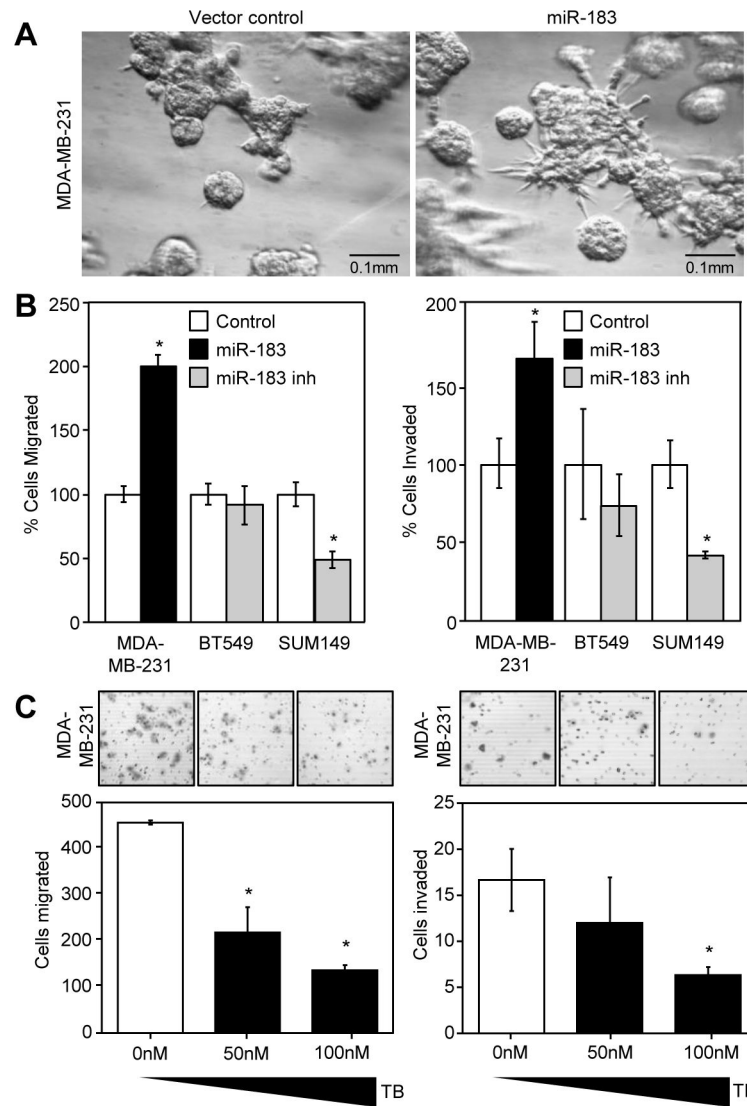


**Figure 6. miR-183 promotes transwell migration and invasion.**

(A) Representative images (20X) vector control and miR-183 transduced MDA-MB-231 cells cultured in Geltrex at 37°C for 6 days. (B) Stable miR-183 overexpressing MDA-MB-231 cells or vector control and miR-183 inhibitor transfected and control inhibitor transfected cells were seeded into 24-well plate control inserts for migration or inserts containing a thin layer of Matrigel for invasion. Cells were allowed to migrate and invade for 16–18hr. Cells per field were quantified.  $n=3$  transwells per group. Data representative of at least 3 independent experiments (C) Stable miR-183 overexpressing MDA-MB-231 cells were transfected with the indicated concentrations of a target site blocker (TB) for the most conserved miR-183 binding site in the SIN3A 3'UTR. 24hr post-transfection cells were seeded into transwells for migration and invasion. Cells were allowed to migrate and invade for 18hr. Representative images are shown, 10X. Error bars Mean  $\pm$  SEM: \* $p<0.05$ , student's t-test.

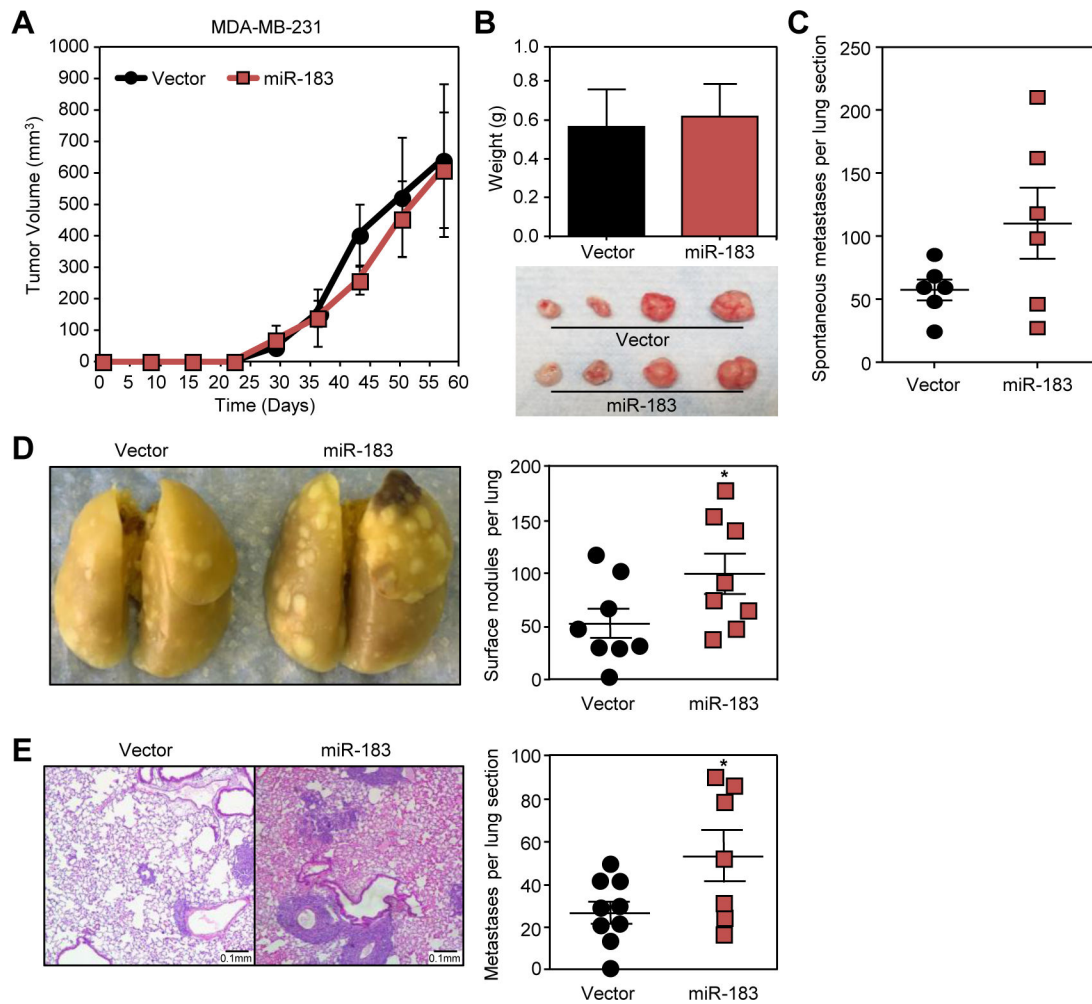


**Figure 7. miR-183 promotes metastasis.**

MDA-MB-231 cells were infected with miR-183-encoded retrovirus or empty retrovirus (vector) control. (A-C) Cells were injected subcutaneously into the flanks of immunocompromised mice. (A) Tumor volume was measured at intervals and (B) tumor weight was measured at time of sacrifice. Error bars indicate SEM. Representative images shown. n=6 mice per group. (C) Mice were evaluated for spontaneous metastases at the time of necropsy. Lungs were fixed and H&E stained. Quantification of spontaneous metastases per section to the lung. (D-E) Cells were injected into the lateral tail vein of immunocompromised mice. Lungs were collected and fixed in Bouin's at the time of sacrifice (D) Quantification of surface lung nodules, representative images of lungs shown (E) Quantification of lung metastases per H&E stained histology section. Representative images shown, 10X. Error bars Mean  $\pm$  SEM: \*p<0.05, student's t-test.